Biochemical and Biophysical Research Communications 437 (2013) 408–412

Contents lists available at SciVerse ScienceDirect

Biochemical and Biophysical Research Communications

journal homepage: www.elsevier.com/locate/ybbrc

Intracellular segment between transmembrane helices S0 and S1 of BK channel α subunit contains two amphipathic helices connected by a flexible loop

Pan Shi [a,b], Dong Li [a], Chaohua Lai [a], Longhua Zhang [a,*], Changlin Tian [a,b,*]

[a] Hefei National Laboratory of Microscale Physical Sciences, School of Life Sciences, University of Science and Technology of China, Hefei, Anhui, 230027, PR China
[b] High Magnetic Field Laboratory, Chinese Academy of Sciences, Hefei, Anhui, 230031, PR China

ARTICLE INFO

Article history:
Received 21 June 2013
Available online 2 July 2013

Keywords:
BK channel
Intracellular segment
Solution NMR
Backbone assignment
Secondary structure
Titration

ABSTRACT

The BK channel, a tetrameric potassium channel with very high conductance, has a central role in numerous physiological functions. The BK channel can be activated by intracellular Ca^{2+} and Mg^{2+}, as well as by membrane depolarization. Unlike other tetrameric potassium channels, the BK channel has seven transmembrane helices (S0–S6) including an extra helix S0. The intracellular segment between S0 and S1 (BK-IS1) is essential to BK channel functions and Asp99 in BK-IS1 is reported to be responsible for Mg^{2+} coordination. In this study, BK-IS1 (44–113) was over-expressed using a bacterial system and purified in the presence of detergent micelles for multidimensional heteronuclear nuclear magnetic resonance (NMR) structural studies. Backbone resonance assignment and secondary structure analysis showed that BK-IS1 contains two amphipathic helices connected by a 36-residue loop. Amide ^{1}H–^{15}N heteronuclear NOE analysis indicated that the loop is very flexible, while the two amphipathic helices are possibly stabilized through interaction with the membrane. A solution NMR-based titration assay of BK-IS1 was performed with various concentrations of Mg^{2+}. Two residues (Thr45 and Leu46) with chemical shift changes were observed but no, or very minor, chemical shift difference was observed for Asp99, indicating a possible site for binding divalent ions or other modulation partners.

1. Introduction

The BK channel is a potassium channel with very high single-channel conductance (100–300 pS) that can be activated by intracellular Ca^{2+} and Mg^{2+} as well as by membrane depolarization [1–6]. BK channels have important roles in many physiological processes, including smooth muscle contraction, mediation of alcohol tolerance, hypertension, potassium secretion, neurotransmitter release and neuronal excitability [7,8]. Additionally, enhanced expression of BK channel α subunits is correlated with a high proliferation rate and malignancy of breast cancer [9]. In mammalian cells, the BK channel is encoded by a single *Slo1* gene. In most tissues, BK channels consist of pore-forming α and regulatory β subunits, which are arranged in a 1:1 stoichiometry [10]. In mammals, there are four members of the BK channel β subunit family; β1–β4. The BK channel belongs to the S4 superfamily of K^+ channels, which is characterized by a positively charged S4 helix in the voltage sensor domain (VSD). The BK channel contains four identical α subunits, each comprising a large intracellular C terminus and seven transmembrane helices (S0–S6). The traditional S1–S6 helices include a VSD (S1–S4) and a pore domain (S5–S6) (Fig. 1A). The S0 helix is located before the S1–S6 helices in the BK channel. Thus, the BK channel has its NH_2 terminus on the extracellular side of the membrane and a long cytosolic intracellular segment (BK-IS1) [11]. The S0 segment, which was hypothesized to be involved in β subunit association, can function in modulating voltage sensitivity and might make direct contact with the VSD [10,12–14]. Therefore, analysis of the structure of BK-IS1 will help us to understand the significance of the extra transmembrane helix S0 and its interaction with the β subunits.

Consistent with the role of key regulator of vital body functions, malfunction of BK channels can lead to many diseases, including hypertension, epilepsy, noise-induced hearing loss and urinary incontinence [15–17]. However, no high-resolution structure of BK channels was available, except a recent report of a cryo-EM structure at a resolution of 17–20 Å [18]. Recently, a 3.0 Å resolution crystal structure of the cytosolic domain of Slo1, including both RCK1 and RCK2, has been determined [19]. Compared to the $K_V1.2$ structure, the transmembrane domains of the cryo-EM BK structure contain an additional structural component, which is likely to account for the unique S0 segment in BK channels, as well

* Corresponding authors. Address: University of Science and Technology of China, Hefei National Laboratory of Microscale Physical Sciences, School of Life Sciences, Hefei, Anhui, 230027, PR China. Fax: +86 551 63600441 (C. Tian).
E-mail addresses: zlhustc@ustc.edu.cn (L. Zhang), cltian@ustc.edu.cn (C. Tian).

0006-291X/$ - see front matter © 2013 Elsevier Inc. All rights reserved.
http://dx.doi.org/10.1016/j.bbrc.2013.06.091

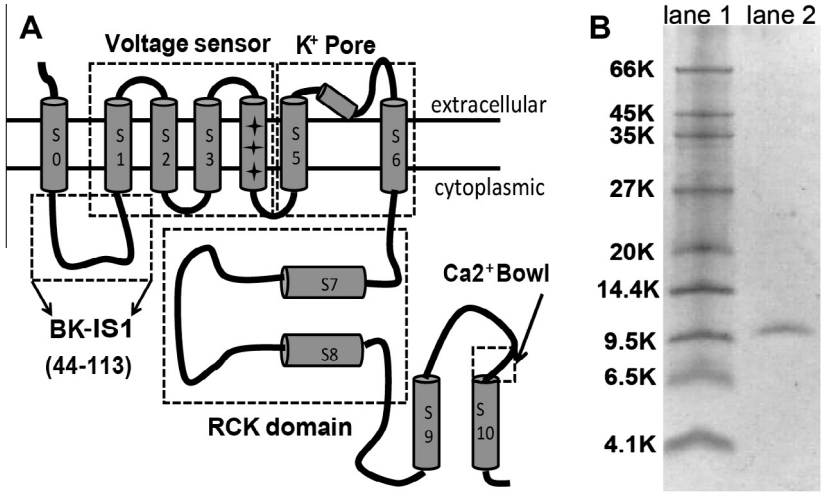

Fig. 1. (A) Diagram of the α subunit of the BK channel [2]. (B) SDS–PAGE of purified human BK-IS1. Lane 1, molecular mass marker; lane 2, purified human BK-IS1.

as the N terminus and BK-IS1 that flank S0 [18]. In addition, it appears that BK-IS1 can form an important component of the interacting region between the BK channel transmembrane domain and the cytosolic RCK domain [6]. Importantly, the BK-IS1 was reported to be engaged in divalent ion-dependent activation of the BK channel. A Mg^{2+}-binding site was mapped at the interface between the VSD (D99 and N172) and the cytosolic domain (E374 and E399) [20,21]. In this study, residue D99 is located in BK-IS1. Several other mutant residues in BK-IS1 have been found to be correlated with diseases: Thr107 of bovine *slo* in BK-IS1 essentially determined the BK channel response to alcohol [22], D81N and D923N in BK-IS1 altered the Ca^{2+} sensitivity of the channel [23]. On the basis of the cryo-EM structure of the BK channel, cytosolic BK-IS1 is proposed to fit snugly between the VSD and the gating ring, filling the void between the core and the C terminus of the gating ring [18]. Therefore, BK-IS1 is crucial in the coupling of voltage sensor and metal ion binding to the activation gate [15]. However, no detailed structural information is available for BK-IS1 concerning divalent ion binding and channel gating.

In this study, over-expressed BK-IS1 was purified and eluted in aqueous buffer containing dodecylphosphocholine (DPC), mimicking lipid bilayer phosphatidylcholine head groups. Once backbone assignments were finalized, the secondary structure and backbone flexibility of BK-IS1 were analyzed and the results showed two helices connected by a flexible loop region. With the availability of sparse nuclear overhauser effect (NOE) restraints, structures of the two helices were calculated to show amphipathic properties. Two consecutive residues in the N terminus of BK-IS1 were observed to have chemical shift perturbations in the two-dimensional NMR spectra upon increased concentration of Mg^{2+}.

2. Materials and methods

2.1. Expression construct

The DNA sequence encoding intracellular segment 1 of the human BK channel (BK-IS1) was amplified using the polymerase chain reaction (PCR) with a pair of primers including *Nde*I restriction enzyme site at the 5′ end and *Xho*I restriction enzyme site at the 3′ end. The amplified fragment was inserted into the pET-21b vector (Novagen Co.) between the two restriction enzyme sites and verified by DNA sequencing. Cysteine residues C53, C54 and C56 were mutated to serine (C53S, C54S and C56S) using a standard PCR-based mutagenesis method and confirmed by DNA sequencing. The mutant expression plasmid was transformed into BL21(DE3) Gold (Novagen Co.). Bacteria were grown in M9 minimal medium containing 100 μg/mL ampicillin. Cultures were grown at 37 °C (with shaking at 225 rpm) until the absorbance at 600 nm (A_{600}) reached 1.0. IPTG was added (final concentration 1 mM) to induce protein expression and the culture was kept at 37 °C (with shaking at 225 rpm) for 4 h.

To achieve over-expression of ^{15}N-labeled BK-IS1, 1.0 g/L [^{15}N]NH_4Cl and 3.0 g/L [^{13}C]glucose (Cambridge Isotope Laboratory, Andover, MA) were added to M9 medium for $^{13}C/^{15}N$ labeling. For expression of only ^{15}N-labeled BK-IS1, the protein was expressed in M9 medium containing 1.0 g/L [^{15}N]NH_4Cl and unlabeled glucose. NH_4Cl and glucose were the only sources of nitrogen and carbon in the M9 medium, respectively.

2.2. Protein purification and on-column refolding in solution containing detergent micelles

Bacterial cells expressing recombinant BK-IS1 were harvested by centrifugation at 4000 rpm for 20 min at 18 °C (Beckman Coulter X-15R). The sediment was collected and suspended in 40 mL of lysis buffer (70 mM Tris–HCl, 300 mM NaCl, pH 8.0) then probe-sonicated (VC500, Sonics and Materials, Danbury, CT) on ice for a total of 10 min (power level, 30%; 2.0 s pulse on and 4.0 s pulse off). 5 mg of Lysozyme, DNase and RNase were added and the lysate was mixed at 4 °C for 1 h then centrifuged at 16,000 rpm for 20 min at 4 °C (Hitachi Himac Centrifuge, CR21GII). The pellet was recovered, suspended in 40 mL of lysis buffer, sonicated and centrifuged again, as described above.

The pellet was suspended in binding buffer (20 mM Tris–HCl, 100 mM NaCl, pH 8.0) containing 8 M urea and 0.2% (w/v) SDS. The suspension was mixed at room temperature for 2 h followed by centrifugation at 16,000 rpm for 20 min at 18 °C (Hitachi Himac Centrifuge, CR21GII). The supernatant was recovered and mixed with 5 mL of Ni^{2+}-NTA resin (QIAgen, Valencia, CA) then mixed at room temperature for 30 min before loading onto a gravity-flow column (BIO-ARD, Hercules, CA) equilibrated with 20 mM Tris–HCl (pH 8.0), 200 mM NaCl. Non-specificity proteins were washed out by elution with 50 mL of 20 mM Tris–HCl, 200 mM NaCl, 8 M urea, 0.2% (w/v) SDS, pH 8.0. Next, 40 mL of washing buffer (20 mM Tris–HCl, 200 mM NaCl, pH 8.0) containing 0.2% (v/v) DPC (Anatrace, Maumee, OH) were used to exchange detergents and to achieve protein on-column refolding. BK-IS1 was eluted with 20 mM Tris–HCl, 200 mM NaCl, 250 mM imidazole, pH 8.0 containing 0.5% DPC. The concentration of purified BK-IS1 was determined via measurement of A_{280} and the purity of BK-IS1

was checked by standard SDS–PAGE. The purified protein was concentrated using an Amicon Ultra-15 device (3000 MWCO, Millipore). Two rounds of concentration of the eluted fraction and dilution into NMR buffer (50 mM NaH_2PO_4/Na_2HPO_4, pH 6.5) were used for buffer exchange and to remove the imidazole. The final volume of the sample was 450 μL and D_2O was added to the concentrated aliquots to a final concentration of 10% (v/v). The protein concentration used for multi-dimensional NMR experiments was about 1.5 mM.

2.3. NMR data acquisition, backbone resonance assignment and structure calculation

Two-dimensional ^1H–^{15}N heteronuclear single quantum correlation spectroscopy (HSQC) experiments for ^{15}N-labeled BK-IS1 samples with DPC micelles were done at 35 °C (500 MHz Bruker spectrometer equipped with a TXI probe). A standard Bruker HSQC pulse sequence was used, with 1024 × 256 complex points in the ^1H and ^{15}N dimensions, respectively. Two-dimensional NMR data were processed using nmrPipe [24] with a gaussian window function for both dimensions and spectra were analyzed and plotted using nmrView [25].

A set of triple resonance multi-dimensional NMR experiments was done for [^{13}C, ^{15}N]BK-IS1 in 50 mM NaH_2PO_4/Na_2HPO_4, 3.5% DPC, pH 6.5, at 35 °C (500 MHz Bruker spectrometer). The NMR experiments included HNCO, HNCA, HN(CA)CO, HNCACB, CBCA(-CO)NH, CC(CO)NH, HCC(CO)NH and HBHA(CO)NH. Data from the triple resonance experiments were processed using nmrPipe with both forward and backward linear prediction to improve resolution in each indirect dimension. The resulting NMR spectra were processed using nmrPipe and analyzed using nmrView for backbone resonance assignment.

The NOE spectroscopy (NOESY) inter-proton distance constraints were derived from the 3D heteronuclear ^{15}N-edited NOESY–HSQC experiments. The initial structure calculations were done with the XPLOR-NIH program.

2.4. Secondary structure calculation and backbone relaxation analysis

Following backbone resonance assignment, the secondary structure of BK-IS1 in the presence of detergent micelles was calculated using the TALOS + program with input of chemical shift values of backbone amide ^1H, ^{15}N, ^{13}CO, $^{13}C_\alpha$, and $^{13}C_\beta$ [26]. The relaxation parameter, the ^1H–^{15}N NOE, for backbone amide ^{15}N nuclei, was acquired at 35 °C (500 MHz Bruker spectrometer). The number of points was 256 and 1024 in the indirect and direct dimensions, respectively. The steady-state ^1H–^{15}N NOE intensities were obtained from the ratio $I_{NOE}/I_{NO\text{-}NOE}$, where I_{NOE} and $I_{NO\text{-}NOE}$ are the peak heights in the NOE spectra with and without proton saturation, respectively.

2.5. Magnesium titration study of BK-IS1

The experiments were done with 1.0 mM [^{15}N]BK-IS1 in DPC micelles. Two-dimensional ^1H–^{15}N HSQC spectra with increased concentration of Mg^{2+} were collected at 35 °C (500 MHz Bruker spectrometer). A series of HSQC spectra was collected for BK-IS1 with protein/Mg^{2+} molar ratios of 1:0, 1:1, 1:5 and 1:20.

3. Results and discussion

3.1. Protein expression and purification

BK-IS1 was over-expressed in *Escherichia coli* BL21(DE3) gold using the bacteriophage T7 promoter system. The wild type BK-IS1 contains three cysteine residues, leading to oligomer formation of the over-expressed protein in *E. coli* (data not shown). To achieve monomeric BK-IS1 for structural studies, the three cysteine residues in the BK-IS1 were mutated to serine to avoid protein aggregation. Because DPC has head groups similar to those of phosphocholine lipids in the cell membrane, BK-IS1 was eluted into DPC for further structural studies using solution NMR. SDS–PAGE analysis of protein purified by Ni^{2+}-NTA affinity chromatography showed a single band, indicating a homogeneous sample, available for solution NMR structural studies (Fig. 1B).

^{15}N and/or ^{13}C labeling of BK-IS1 was achieved by growing the protein in defined M9 medium containing [^{15}N]NH_4Cl as sole nitrogen source or [^{13}C]glucose as sole carbon source.

3.2. NMR backbone resonance assignment

A two-dimensional ^1H–^{15}N HSQC spectrum with good signal dispersion was obtained at 35 °C for BK-IS1 in DPC micelles. Series of two- and three-dimensional solution NMR spectra were acquired for sequential backbone resonance assignment. Backbone amide (N)H, N, C_α, C_β and CO chemical shifts were assigned for 61 residues out of Pro79 and 69 non-proline residues in BK-IS1 (Fig. 2A). Side chain resonance assignments were made for BK-IS1 in DPC micelles using ^{15}N-edited NOESY-HSQC experiments to obtain NOE distance restraints for structure calculation.

3.3. Secondary structure calculation

After backbone resonance assignment, the chemical shift values of BK-IS1 ((N)H, N, C_α, C_β, and CO) were analyzed using the TALOS + program for secondary structure prediction [26]. The predicted secondary structure for all residues of BK-IS1 are shown in Fig. 3A (upper panel), where the negative bars indicate α-helix secondary structure and positive bars indicate a β-strand. This result demonstrated that BK-IS1 contains two helical segments (R44–S56 and W93–L110) connected by a random coil region (G57–G92).

Heteronuclear ^1H–^{15}N NOE were acquired (500 MHz Bruker spectrometer) to characterize the backbone dynamics of BK-IS1. Residues R44–S56 and W93–L110 showed positive NOE values $\geqslant 0.5$ and residues G57–A89 displayed negative NOE values, indicating that two relatively rigid regions within the secondary structure are connected by a loop with great flexibility. The heteronuclear NOE data were highly consistent with the TALOS + predicted secondary structure of BK-IS1 (Fig. 3A).

3.4. Structural calculation of BK-IS1

The structure of BK-IS1 in detergent micelles was calculated using Xplor-NIH on the basis of the dihedral restraints predicted by TALOS + and the ^{15}N-NOE restraints. Statistics for the restraints and the structure quality are summarized in Table 1. The final structure showed two converged helices at NH_2 and C terminal of BK-IS1 (Fig. 3B). Owing to the limited number of structural restraints, structural convergence was not as good as that for other soluble proteins. Side and top views of helix 1 (residues R44–S56) are shown in Fig. 3B and the side view of helix 2 (residues W93–L110) is shown in Fig. 3C. Both helical segments are amphipathic, with hydrophobic residues located on one side and hydrophilic residues on the other side, providing strong hints that the two amphipathic helices probably interact with the membrane by lying on the hydrophobic/hydrophilic interface of lipid bilayers, which is consistent with the relatively rigid backbone of the two helices identified from the heteronuclear ^1H–^{15}N NOE data. Because the central segment was predicted to be random coil with

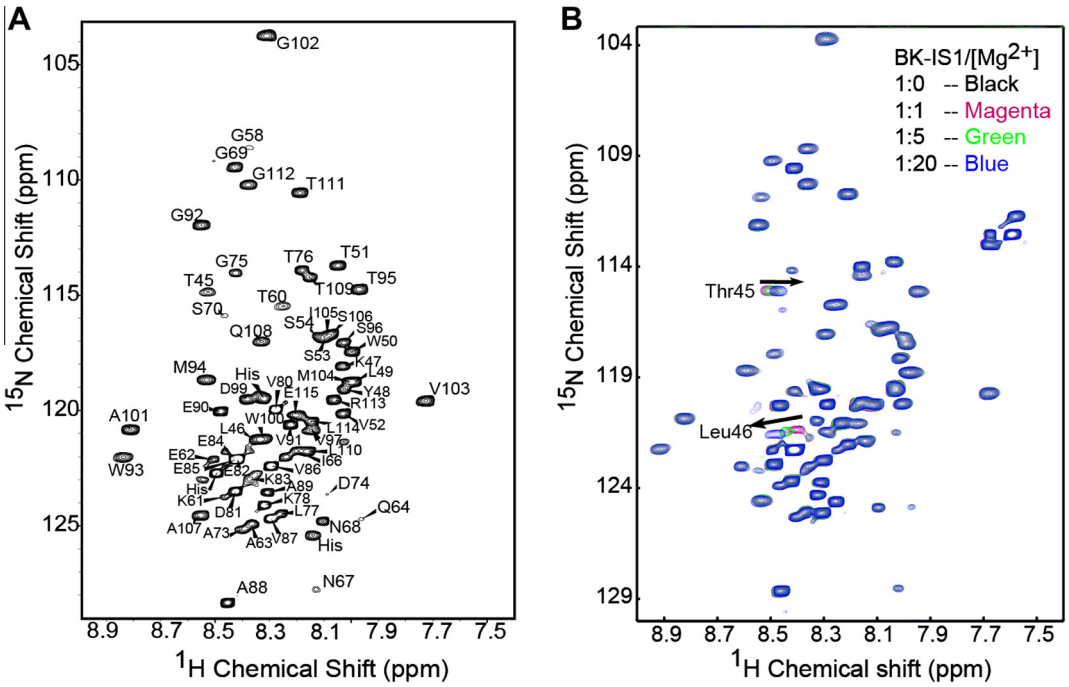

Fig. 2. (A) The solution NMR backbone resonance assignment of BK-IS1 in DPC micelles in 50 mM NaH_2PO_4/Na_2HPO_4, pH 6.5; 61 of the 69 non-proline residues of BK-IS1 (44–113) were assigned. (B) Chemical shift perturbations of BK-IS1 in DPC micelles with different protein/Mg^{2+} molar ratios.

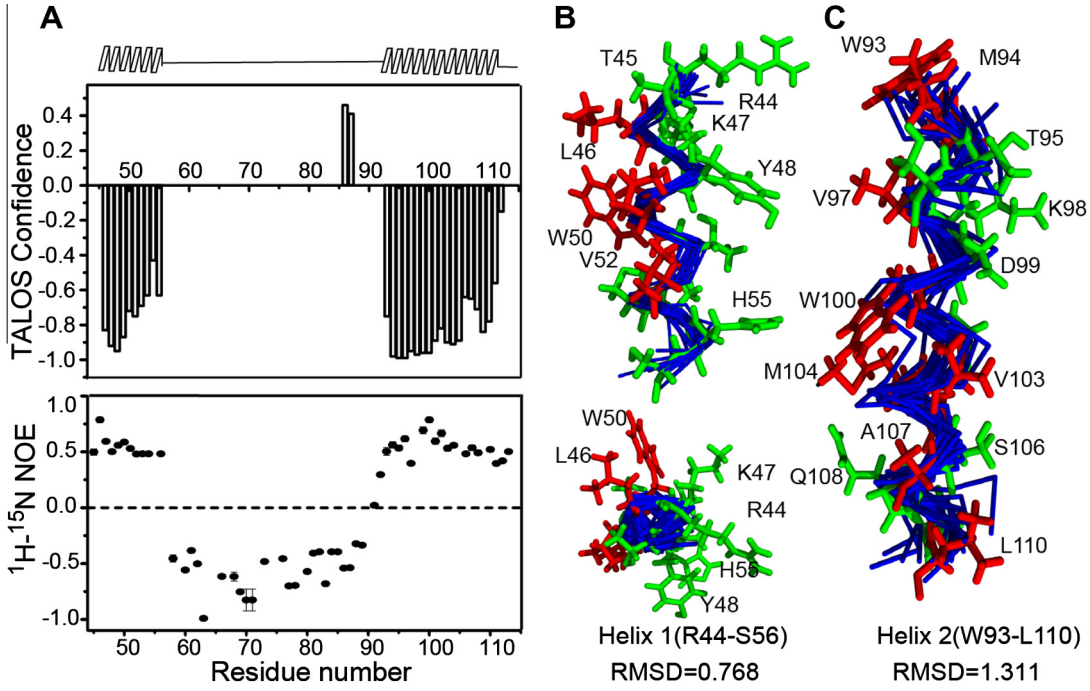

Fig. 3. (A) TALOS + secondary structure calculation based on chemical shift values of BK-IS1((N)H, N, ^{13}CO, $^{13}C_\alpha$ and $^{13}C_\beta$). Negative chemical shift index (CSI) values indicate secondary structures of α-helix and positive CSI values indicate β-strand. The secondary structure analysis of BK-IS1 (upper panel) is consistent with the heteronuclear ^{1}H–^{15}N NOE data (below). (B) Side and top views of the amphipathic helix 1 (R44–S56). (C) Side view of amphipathic helix 2 (W93–L110). The backbone atoms are shown in blue, and the side-chains of hydrophilic and hydrophobic residues are shown in green and red, respectively. (For interpretation of the references to colour in this figure legend, the reader is referred to the web version of this article.)

negative ^{1}H–^{15}N heteronuclear NOE values, no converged structure of the segment between G57 and G92 could be obtained.

3.5. Magnesium titration study of BK-IS1

Earlier, Asp99 was reported to have an important role in coordinating Mg^{2+}, together with residues from the RCK domain of the BK channel. In this study, a solution NMR titration assay of BK-IS1 in the presence of DPC micelles was done with increased concentration of Mg^{2+}. Two-dimensional HSQC spectra of BK-IS1 with different protein/Mg^{2+} molar ratios (1:0, 1:1, 1:5 and 1:20) are shown in Fig. 2B. Only Thr45 and Leu46 in the overlaid spectra were observed to have progressive chemical shift perturbations with increased concentration of Mg^{2+}. To our surprise, very minor

Table 1
Summary of statistics for the 20 final structures of BK-IS1 (44–113).

Structural restraints	
NOE distance restraints	145
Intraresidue ($i = j$)	172
Sequential ($\|i - j\| = 1$)	93
Medium-range ($2 \leqslant \|i - j\| \leqslant 4$)	41
Long-range ($\|i - j\| \geqslant 5$)	0
TALOS dihedral angle constraints	98
Total	549
Coordinate precision	
RMSD to the mean (Å)	Backbone/Heavy atoms
Residues in helix 1 (44–56)	0.7686/1.673
Residues in helix 2 (93–110)	1.311/2.143
Ramachandran plot statistics (%)	
Most-favored regions	77.2
Additionally allowed regions	15.7
Generously allowed regions	5.5
Disallowed regions	1.6

or no progressive chemical shift change was observed for D99, probably because the single D99 residue cannot provide suitable coordinates to stabilize Mg^{2+}, which requires cooperative behavior of D99, N172, E374 and E399 residues[20].

Although Thr45 and Leu46 are consecutive and located at the N terminus of BK-IS1, they showed different chemical shift responses with increased concentration of Mg^{2+} (Fig. 2B). The chemical shift of Thr45 moved to high field, whereas the chemical shift of Leu46 moved progressively to low field, indicating some specific interactions between the NH_2 terminal of BK-IS1 and Mg^{2+}. Surprisingly, titration of BK-IS1 with the C terminal tails of the β2 subunits of the BK channel also showed chemical shift perturbations of these two residues (Fig. S1). These observations implied that these two residues have important roles in functional modulation of the BK channel by either divalent ions or β subunit proteins.

Acknowledgments

We thank Mr. Jiahai Zhang for his maintenance of the solution NMR spectrometers in the University of Science and Technology of China. This work was supported by the Chinese Key Research Plan (No. 2011CB911104 and 2006CB910204) to C.T. and Chinese Natural Science Foundation (No. 31100847) to L.Z.

Appendix A. Supplementary data

Supplementary data associated with this article can be found, in the online version, at http://dx.doi.org/10.1016/j.bbrc.2013.06.091.

References

[1] M. Prakriya, C.J. Lingle, BK channel activation by brief depolarizations requires Ca^{2+} influx through L- and Q-type Ca^{2+} channels in rat chromaffin cells, J. Neurophysiol. 81 (1999) 2267–2278.
[2] R. Latorre, S. Brauchi, Large conductance Ca^{2+}-activated K^+ (BK) channel: activation by Ca^{2+} and voltage, Biol. Res. 39 (2006) 385–401.
[3] J. Shi, G. Krishnamoorthy, Y. Yang, L. Hu, N. Chaturvedi, D. Harilal, J. Qin, J. Cui, Mechanism of magnesium activation of calcium-activated potassium channels, Nature 418 (2002) 876–880.
[4] X.M. Xia, X. Zeng, C.J. Lingle, Multiple regulatory sites in large-conductance calcium-activated potassium channels, Nature 418 (2002) 880–884.
[5] J. Shi, J. Cui, Intracellular Mg^{2+} enhances the function of BK-type Ca^{2+}-activated K^+ channels, J. Gen. Physiol. 118 (2001) 589–606.
[6] H. Yang, L. Hu, J. Shi, K. Delaloye, F.T. Horrigan, J. Cui, Mg^{2+} mediates interaction between the voltage sensor and cytosolic domain to activate BK channels, Proc. Natl. Acad. Sci. USA 104 (2007) 18270–18275.
[7] G.J. Kaczorowski, H.G. Knaus, R.J. Leonard, O.B. McManus, M.L. Garcia, High-conductance calcium-activated potassium channels; structure, pharmacology, and function, J. Bioenerg. Biomembr. 28 (1996) 255–267.
[8] B.S. Rothberg, The BK channel: a vital link between cellular calcium and electrical signaling, Protein Cell 3 (2012) 883–892.
[9] M. Oeggerli, Y. Tian, C. Ruiz, B. Wijker, G. Sauter, E. Obermann, U. Guth, I. Zlobec, M. Sausbier, K. Kunzelmann, L. Bubendorf, Role of KCNMA1 in breast cancer, PLoS one 7 (2012) e41664.
[10] L. Toro, M. Wallner, P. Meera, Y. Tanaka, Maxi-K(Ca), a unique member of the voltage-gated K channel superfamily, News Physiol. Sci. 13 (1998) 112–117.
[11] G. Liu, S.I. Zakharov, L. Yang, S.X. Deng, D.W. Landry, A. Karlin, S.O. Marx, Position and role of the BK channel alpha subunit S0 helix inferred from disulfide crosslinking, J. Gen. Physiol. 131 (2008) 537–548.
[12] O.M. Koval, Y. Fan, B.S. Rothberg, A role for the S0 transmembrane segment in voltage-dependent gating of BK channels, J. Gen. Physiol. 129 (2007) 209–220.
[13] M. Wallner, P. Meera, L. Toro, Determinant for beta-subunit regulation in high-conductance voltage-activated and Ca^{2+}-sensitive K^+ channels: an additional transmembrane region at the N terminus, Proc. Natl. Acad. Sci. USA 93 (1996) 14922–14927.
[14] P. Meera, M. Wallner, M. Song, L. Toro, Large conductance voltage- and calcium-dependent K+ channel, a distinct member of voltage-dependent ion channels with seven N-terminal transmembrane segments (S0–S6), an extracellular N terminus, and an intracellular (S9–S10) C terminus, Proc. Natl. Acad. Sci. USA 94 (1997) 14066–14071.
[15] U.S. Lee, J. Cui, BK channel activation: structural and functional insights, Trends Neurosci. 33 (2010) 415–423.
[16] G.C. Amberg, L.F. Santana, Downregulation of the BK channel beta1 subunit in genetic hypertension, Circ. Res. 93 (2003) 965–971.
[17] J. Cui, H. Yang, U.S. Lee, Molecular mechanisms of BK channel activation, Cell. Mol. Life Sci. 66 (2009) 852–875.
[18] L. Wang, F.J. Sigworth, Structure of the BK potassium channel in a lipid membrane from electron cryomicroscopy, Nature 461 (2009) 292–295.
[19] P. Yuan, M.D. Leonetti, A.R. Pico, Y. Hsiung, R. MacKinnon, Structure of the human BK channel Ca^{2+} -activation apparatus at 3.0 A resolution, Science 329 (2010) 182–186.
[20] H. Yang, J. Shi, G. Zhang, J. Yang, K. Delaloye, J. Cui, Activation of Slo1 BK channels by Mg^{2+} coordinated between the voltage sensor and RCK1 domains, Nat. Struct. Mol. Biol. 15 (2008) 1152–1159.
[21] R.S. Chen, Y. Geng, K.L. Magleby, Mg^{2+} binding to open and closed states can activate BK channels provided that the voltage sensors are elevated, J. Gen. Physiol. 138 (2011) 593–607.
[22] J. Liu, M. Asuncion-Chin, P. Liu, A.M. Dopico, CaM kinase II phosphorylation of slo Thr107 regulates activity and ethanol responses of BK channels, Nat. Neurosci. 9 (2006) 41–49.
[23] A.P. Braun, L. Sy, Contribution of potential EF hand motifs to the calcium-dependent gating of a mouse brain large conductance, calcium-sensitive K^+ channel, J. Physiol. 533 (2001) 681–695.
[24] F. Delaglio, S. Grzesiek, G.W. Vuister, G. Zhu, J. Pfeifer, A. Bax, NMRPipe: a multidimensional spectral processing system based on UNIX pipes, J. Biomol. NMR 6 (1995) 277–293.
[25] B.A. Johnson, Using NMRView to visualize and analyze the NMR spectra of macromolecules, Methods Mol. Biol. 278 (2004) 313–352.
[26] Y. Shen, F. Delaglio, G. Cornilescu, A. Bax, TALOS+: a hybrid method for predicting protein backbone torsion angles from NMR chemical shifts, J. Biomol. NMR 44 (2009) 213–223.